Coupling of electrodynamic fields to vibrational modes in helical structures

Asaf Farhi and Aristide Dogariu

Phys. Rev. A **103**, 023523 — Published 19 February 2021

DOI: 10.1103/PhysRevA.103.023523

Coupling electrodynamic fields to vibrational modes in helical structures

Asaf Farhi and Aristide Dogariu
CREOL, University of Central Florida, Orlando, Florida, USA 32816

Helical structures like alpha helices, DNA, and microtubules have profound importance in biology. It has been suggested that these periodic arrangements of constituent units could support collective excitations similarly to crystalline solids. Here, we examine the interaction between such constructs and oscillating dipoles, and evaluate the role of the helicity in the coupling between electrodynamic fields and vibrations. Based on a vibrational and eigenfunction analyses we identify a group of modes of coherent oscillations that give rise to a strong and delocalized response, selectivity in frequency, and typical interaction range. To describe the field scattering due to the structure vibrations we consider an anisotropic permittivity with a helical periodicity, which applies to all vibration types and close dipole locations. This new type of resonances identified here may help explain the role of electrodynamic fields in the diverse functionality of cytoskeletal microtubules in the cellular environment.

PACS numbers:

I. INTRODUCTION

Microtubules (MTs) are tubular helical structures that self-assemble from their constituent tubulin-protein units. MTs are critical for the development and maintenance of the cell shape, transport of vesicles and other components throughout cells, cell signaling, and mitosis. Tubulins have a large dipole moment [1–4] and it was conjectured that MT vibrations could generate electric field in its vicinity [5-7], also beyond the typical Coulomb and vdW range. This process can be powered by GTP hydrolysis, motor proteins that move along the MT, and mitochondria energy release [6]. MTs were also analyzed in the context of robust-edge topological vibrational modes [8], vibrational modes of hollow-cylinders, and two-dimensional (2D) crystal lattices [9-10]. Recently, their 3D mechanical vibrations were calculated numerically using a molecular structural-mechanics model [11] and their acoustic modes were measured experimentally under the assumption of thermal equilibrium [12]. Importantly, alternating electric fields were shown to inhibit cancerous cell-growth by an anti-MT mechanism [13].

MTs have a highly regular helical shape that is rare in nature, similarly to carbon nanotubes [14]. Their constituent units are identical, even more than in DNA and alpha helices, whose elementary units have different residues. In addition, the MT structure appears like a shifted crystal, which may give rise to axial propagation of vibrations. It is certainly of interest to understand how this exquisite geometry may affect oscillatory phenomena of MTs such as vibrations and electromagnetic (EM) excitations. In a broader sense, one can ask if these properties are critical for the diverse functionality of MTs in biology. Of particular interest would be to understand the interaction with surrounding molecules and if the modes have a particular extent and frequency properties.

In the following, we answer these questions to some extent. We first analyze vibrations in a helical structure by employing a top-view model that describes accurately macroscopic vibrations of complex structures. We then develop an eigenfunction analysis [15–18] for the vibrational-mode-mediated interaction between a MT and an oscillating electric dipole in a host medium. To that end, we consider an infinitely-long dielectric structure in a uniform medium, which applies to MTs and DNAs that have a persistence length much larger than the radius and is an approximation for alpha helices that have a persistence length of 1nm and a radius of 2.3Å [19]. The dielectric structure consists of units disposed in a helical arrangement that can vibrate in a collective manner and have internal vibrational and electronic excitations. We will focus on properties that arise from the helical arrangement and even though the units in MTs, DNAs, and alpha helices are different, the analysis should apply to most cases. In addition, while the structure vibrations can be damped by the medium, the vibrations of a cylindrical-shell-medium system can behave similarly to a free shell [9]. A dipole in proximity to this structure emits radiation with a wavelength $\lambda = 2\pi c/\omega \gg l$, where l is the typical length scale, and therefore the interaction can be analyzed in the quasistatic approximation [20]. In this regime, the electric and magnetic fields are decoupled and the electric field, which oscillates in time, obeys Poisson's equation [15–17]. We derive eigenfunctions that express the scattering of the electric field due to the vibrations. To descibe this interaction, we define the MT as an inclusion with a permittivity $\overleftrightarrow{\epsilon_1}(\omega, \mathbf{r})$ that is anisotropic and periodic along a helical orbit, and the host-medium with a permittivity $\epsilon_2(\omega)$, assuming $\omega > 250$MHz, in which ionic screening is negligible [2].

II. RELATING THE VIBRATIONS TO THE INCOMING-FIELD MODES

We consider a dipole that emits radiation, which impinges on the helical structure. In the near field, the

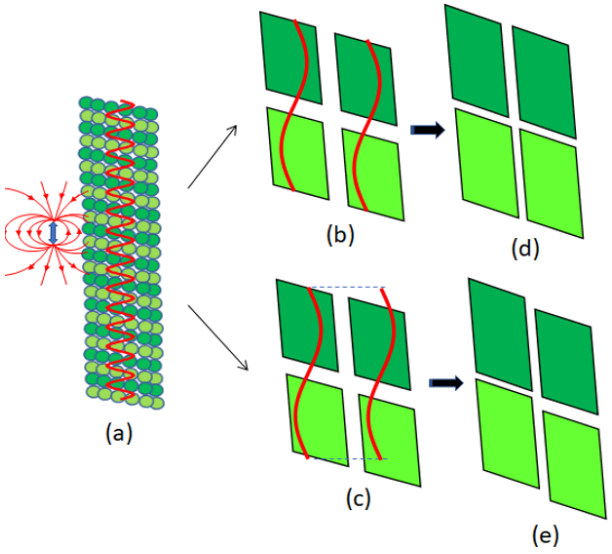

Figure 1: The physical system: an oscillating dipole emitting electromagnetic field is in proximity to a microtubule. Part of the electric field couples to vibrational modes in the microtubule (a). The coupled field can be in a helical arrangement (b) or standard longitudinal arrangement (constant when varying the azimuthal angle) (c). In response to the field, the tubulins deform and translate such that they move synchronously (d) or asynchronously (e).

dominant spatial frequencies of the emitted field correspond to wavelengths on the order of the distance from the dipole [17, 21]. We define the incoming field $\mathbf{E}^{\text{inc}}$ as the dipole field in a uniform ϵ_2 medium [15–17]. While this field is usually described with respect to the dipole position, we utilize its expansion with respect to the structure axis to relate it to the structure vibrations. We consider the case in which laterally-adjacent units move together, that for an axially-shifted crystal results in that each axial chain behaves as a 1D crystal. To impose this movement, we require $\mathbf{E}^{\text{inc}}$ to be symmetric to a continuous translation along a helical orbit. This situation is illustrated in Fig. 1 (a) for the case of a MT, in which the tubulin dimers are disposed in a helical arrangement. The electric fields in helical and longitudinal configurations are shown in Fig. 1 (b) and (c). As a result, the tubulin units can change their size and move as suggested in (d) and (e), respectively. In a helical-field arrangement, laterally-adjacent units move together (d). The movement where the adjacent tubulins are not aligned as shown in Fig. 1 (e) is assumed to be less favorable energetically. Imposing this symmetry on $\mathbf{E}^{\text{inc}}$ inside the structure results in (see Appendix (A) 1)

$$\mathbf{E}^{\text{inc}}(\phi, z, \rho) \propto \exp\left(im\left(\phi - k_z z\right)\right) \tag{1}$$

where m is an integer number, $k_z = 2\pi/a$, a is the helical-orbit axial period, and ϕ, z, ρ are cylindrical-coordinates variables. In these field modes, the k and m degrees of freedom are related by $k = mk_z$, which, if the medium responds strongly to them, implies selectivity in $\mathbf{k}$ and ω. Clearly, the high-m modes have high spatial frequencies and can be dominant only for close dipole locations. In addition, invariance of $\mathbf{E}^{\text{inc}}$ to discrete lateral translations along the helix results in the same field distribution in each constituent unit and a coordinated movement. Such modes have high spatial frequencies $k_z n$, where n is the number of units per helical round. These modes can be excited when the dipole is very close to the helical structure (typical interaction distance is $2\pi/k_z n$) and the field impinging on the structure has very high spatial frequencies. This situation is similar to the simpler case of the electrostatic field generated by charges in a helical arrangement with a uniform-inclusion permittivity [22].

III. VIBRATIONAL-MODE ANALYSIS

Having analyzed the coupling of incoming EM fields to synchronous vibrations, we examine now in more detail the vibrations in the helical structure. We first consider the forms of vibration. Radial movements are expected to be damped [6] since they involve movements of a relatively large volume of liquid. While vibrations of a helical structure are different from vibrations of a spring, a spiral motion may also be less favorable mechanically since it involves movements of long helical chains. Moreover, in the context of MTs, the azimuthal dipole moment is small [6] and in a recent work torsion was found to be insignificant [11]. We will therefore focus on axial vibrations.

We now analyze classically the vibrational modes that can be excited by the incoming field and generate field. For 1D crystals, such a treatment agrees with the quantum analysis [25]. We consider the coupling of vibrations also to field components with $kc \gg \omega$ that are almost static [26]. While interaction of near field with a crystal was analyzed for $ka \ll 1$ [27, 28], we extend it to $ka \geq 1$. When vibrational modes and electric field are coupled they have the same $\omega, \mathbf{k}$, and at low and high ks, $\omega(k)$ of one of the polaritons and the uncoupled vibrational mode are similar [25]. We also show that in our case the 1D crystal symmetry $k \rightarrow k + k_z$ [25] is not satisfied. We consider a structure comprising two types of units with masses m_1, m_2 connected by springs k_1, k_2, k_3, k_4 as shown in Fig. 2 (b). Denoting the axial displacements of $m_{1,2}$ and the indices of the axial and lateral shifts by $u_{1,2}$ and s, q, respectively, and assuming $u_{1,2} = a_{1,2}e^{ikz+im\phi}$, we write the equations of motion (EOM)

$$
\begin{aligned}
-\omega^2 m_1 u_{1sq} =& k_1\left(u_{2sq}-u_{1sq}\right)-k_2\left(u_{1sq}-u_{2s-1q}\right)-k_3\left(u_{1sq}-u_{1sq+1}\right)-k_3\left(u_{1sq}-u_{1sq-1}\right),\\
-\omega^2 m_2 u_{2sq} =& k_2\left(u_{1s+1q}-u_{2sq}\right)-k_1\left(u_{2sq}-u_{1sq}\right)-k_4\left(u_{2sq}-u_{2sq+1}\right)-k_4\left(u_{2sq}-u_{2sq-1}\right),
\end{aligned}
\tag{2}
$$

$$
\begin{pmatrix} -\omega^2 m_1+k_1+k_2+4k_3\sin^2\left(\left(ka/n-2\pi m/n\right)/2\right) & -\left(k_2e^{-ika}+k_1\right)\\ -\left(k_2e^{ika}+k_1\right) & -\omega^2 m_1+k_1+k_2+4k_4\sin^2\left(\left(ka/n-2\pi m/n\right)/2\right)\end{pmatrix}\begin{pmatrix}u_1\\u_2\end{pmatrix}=\begin{pmatrix}0\\0\end{pmatrix}.
\tag{3}
$$

This *1D description* enables us to analyze the behavior of the system in the axial axis while accounting implicitly for the lateral interactions in the terms with k_3, k_4. These diagonal terms with k_3, k_4 restrain the movements of m_1, m_2 to their sites as in a local oscillator and vanish for the helical functions satisfying $k = mk_z$ (see Eq. (1)). These interactions are associated with propagation of axial movements along a helical orbit similarly to an infinite chain of identical particles [25].

For the $k = mk_z$ modes since $u_{1s,q+1} = u_{1s,q}e^{i(ka/n-2\pi m/n)}$, laterally adjacent units oscillate in-phase and form a standing wave, resulting in superradiance and strong scattering in some cases [29, 30], [25] p. 102. In more complex structures the identical atoms and therefore the centers of mass of all the units move together, which relates this type of model also to low ω/large mass vibrations. Eq. (3) can be written as $A\mathbf{u} = \omega^2\mathbf{u}$, where A is a Hermitian matrix and therefore diagonalizable. Since ω^2 is real and positive, we obtain $\omega(k)$, which means that the modes are delocalized. We now consider the response at a given $\mathbf{k}$ and therefore analyze the EOM at this $\mathbf{k}$. When anharmonicity or dissipation are incorporated, the matrix formulation and Hermiticity do not hold and localization can arise. We introduce anharmonicity in the axial forces between lateral units due to the alignment shift of the units upon movement. The sum of these (second order) forces $\propto u_{1sq}^2\left[1-2\cos\left(ka/n-2\pi m/n\right)+\cos\left(2\left(ka/n-2\pi m/n\right)\right)\right]$ and translates to an *on-site* term. For the $k = mk_z$ modes these forces vanish and the $u_1 - u_2$ coupling terms are maximal. Moving away from $k = mk_z$ increases the ratio of anharmonicity to dispersion, leading to a more localized response, similarly to interacting diatomic molecules with *internal* anharmonicity [31, 32] (see A.2.1). In A.2.2 we perform a similar analysis for two helical structures without axial periodicity and axial interactions and obtain similar properties. Such properties were recently observed in DNA [29]. We also analyze the effect of dissipation by introducing $\gamma\dot{u}_{1,2}$ terms, which shows that $\mathrm{Re}(\omega(k))$ is hardly affected and $\mathrm{Im}(\omega(k))$ is *constant* at all ks, except at large γs that suppress the acoustic modes (A.2.3). Since we consider axial vibrations and in Ref. [9] the vibrations of a cylindrical-shell-water system behave similarly to a free shell for our $m \geq 1$ modes, we assume that anharmonicity is a more dominant effect at least for the optical modes.

Interestingly, the α, β units of the MT have electrical charges with the same sign [1]. This may imply that "acoustic" modes, for which adjacent units move together [25], generate current and couple to electric field along with optical modes. From Eq. (3) we calculate $\omega(k)$ for the acoustic and optical modes. We find that the $k = mk_z$ modes have the same $\omega(k)$ of a 1D crystal (see Fig. 2 (c) and videos) in agreement with the previous analysis in Eq. (1). In addition, one can substitute $\omega_T \to \omega(\mathbf{k})$ in the expression for ϵ [25] and obtain $\epsilon(\omega, \mathbf{k}) = 1 + 4\pi Nq^2/[m_r(\omega^2(\mathbf{k}) - \omega^2)]$, where q is the charge, m_r is the reduced mass, and N is the charge concentration.

Moreover, the $k = mk_z$ field modes have the same potential distribution in each dimer and for a fixed dimer length (corresponds to internal vibrations or acoustic modes) the dimers can be treated as non-interacting also in the axial axis that may result in a similar spectrum for a dimer and the structure, which agrees with Ref. [34].

IV. QUANTITATIVE ANALYSIS OF THE DIPOLE-STRUCTURE INTERACTION

Having described the vibrational modes of the helical structure, we now examine the scattering of the electric field due to these vibrations. To this end, we will use the eigenstates ψ_k of the quasi-electrostatic potential. In a composite medium ψ_k represents the potential of a field that exists without a source for an inclusion eigenpermittivity ϵ_{1k}. ψ_ks can be used to expand the scattered electric field ψ_{sc}, which is generated due to the existence of the inclusion. In turn, ϵ_{1k}s are calculated by imposing field boundary conditions and depend on the inclusion geometry. For propagating waves, this requires gain and constructive interference as in a laser. However, for evanescent waves ϵ_{1k}s are real and can be reached more naturally. When the inclusion permittivity $\epsilon_1 \approx \epsilon_{1k}$, a physical resonance occurs and the system responds resonantly [15–17].

Let us describe ψ_{sc} for an anisotropic inclusion permittivity with a helical periodicity, which enables us to account for surface roughness. We first associate the permittivity *tensor* to axial vibrations by considering an anisotropic inclusion with an axial permittivity $\epsilon_z(\mathbf{r})$ and $\epsilon_\rho = \epsilon_\phi = \epsilon_2$. We then utilize the structure symmetries to analyze a permittivity with helical periodicity. In crystals, the permittivity is usually expanded in a Fourier

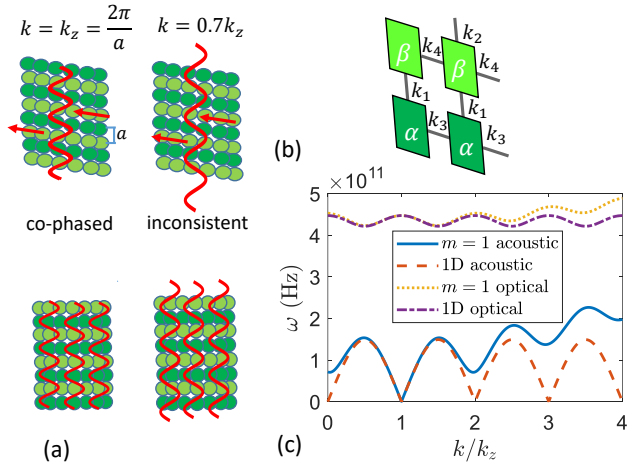

Figure 2: Vibrational-mode analysis for a helical structure. The illustrations show that when varying the field along a helical trajectory, the field coincides with its initial state for $k = k_z m$, implying that these modes are allowed when requiring decoupling between the axial protofilaments (a). The structure is composed of two units denoted by α, β with masses m_1, m_2 connected with springs k_1, k_2, k_3, k_4 (b). $\omega(k)$ for the acoustic and optical $m = 1$ helix and 1D crystal modes. The MT parameters are $m_1 = m_2 = 0.9 \cdot 10^{-22}$ (Kg), $k_1 = 8, k_2 = 1, k_3 = k_4 = 2$ (N/m), $n = 13$, where k_4 is of the order of magnitude of the value in Ref. [10]. (c)

series and it couples each field mode with the modes with $\mathbf{k} + \mathbf{G}_n$, where $\mathbf{G}_n$ is a reciprocal-lattice vector, and there is an effective $\overleftrightarrow{\epsilon_1}(\omega, \mathbf{k})$ that describes the $\omega, \mathbf{k}$ response to an excitation at $\omega, \mathbf{k}$ [15, 20, 26, 35–40]. In our case, the symmetry to discrete translations defines the $k = mk_z$ and $k = nk_z$ modes that represent the "DC" and higher-order Fourier components, respectively. Thus, the coupling is to modes with integer multiples of $(\Delta m, \Delta k) = (1, k_z)$ and $\Delta k = nk_z$ apart. This form of $\overleftrightarrow{\epsilon_1}(\omega, \mathbf{k})$ is justified for the MT because $\lambda/a \gg 1$ and $\rho_{\text{ext}}(\omega) = 0, \mathbf{J}_{\text{ext}}(\omega) = 0$ inside the inclusion, since the charges oscillate only in response to external excitations [26, 41, 42].

We now turn to the quantitative analysis of the dipole-helical structure interaction. In A.3 we show that for $\epsilon_z(\mathbf{k})$ and $\epsilon_\rho = \epsilon_\phi = \epsilon_2$, the amplitude of ψ_k in the expansion of ψ_{sc}, $C_{\mathbf{k}\omega} \propto (\epsilon_2(\omega) - \epsilon_{1z}(\boldsymbol{k}, \omega)) / (\epsilon_{1z\boldsymbol{k}} - \epsilon_{1z}(\boldsymbol{k}, \omega)) \int \theta_1 d\boldsymbol{r} \partial \psi^*_{\boldsymbol{k}} / \partial z E^{\text{inc}}_{\boldsymbol{k}z}$, where $\theta_1 = 1$ in the ϵ_1 volume, and therefore $\boldsymbol{E}^{\text{inc}}_{\boldsymbol{k}}$ results in a contribution of $\psi_{\mathbf{k}}$ with the same $\boldsymbol{k}$ in the expansion. Thus, we write the ψ_ms that describe the spatial dependency of ψ_{sc} due to the $k = mk_z$ vibrations

$$\psi_m = e^{im(\phi - k_z z)} \begin{cases} A_{1m} K_m(mk_z\rho) & \rho > \rho_2 \\ A_{2m} I_m + A_{3m} K_m & \rho_1 < \rho < \rho_2 \\ A_{4m} I_m(mk_z\rho) & \rho < \rho_1 \end{cases}, \quad (4)$$

where ρ_1, ρ_2 are the internal and external inclusion radii, K_m and I_m are the modified Bessel functions. We then solve Laplace's equation in cylindrical coordinates in $\rho_1 < \rho < \rho_2$ to find the argument of the functions

$$\epsilon_2 \frac{1}{\rho} \frac{\partial}{\partial \rho} \left(\rho \frac{\partial \psi_m}{\partial \rho} \right) - \epsilon_2 m^2 \frac{1}{\rho^2} \psi_m - k_z^2 m^2 \epsilon_{zm} \psi_m = 0, \quad (5)$$

and obtain $I_m(mk_z\sqrt{\epsilon_{1zm}/\epsilon_2}\rho)$ and $K_m(mk_z\sqrt{\epsilon_{1zm}/\epsilon_2}\rho)$. To simplify $C_{\mathbf{k}\omega}$ we show in A.3 that the integral in $C_{\mathbf{k}\omega} \propto \epsilon_2(\omega)/(\epsilon_2(\omega) - \epsilon_{1z\boldsymbol{k}}) \nabla \psi^*_{\boldsymbol{k}}(\boldsymbol{r}_0) \cdot \boldsymbol{p}$, where $\mathbf{p}$ is the dipole moment, and $\mathbf{r}_0$ is the dipole location.

Let us now analyze the scaling of ψ_m for small and large ρs. We first observe that the $m = 0$ mode is constant everywhere and can therefore be omitted. This mode is, however, relevant in the far field. For an infinite cylinder, when $k = m = 0$ and $\rho_2 \ll \lambda$, it has the form outside the structure for $k\rho \gg 1$ of $E^{\text{TM}}_{z,m=0} \propto \sqrt{k_0/\rho} e^{i(k_0\rho - \pi/4)}$, where $k_0 = \omega/c$ [23]. Interestingly, this mode extends far from the helical structure and scales as $\sqrt{k/\rho}$. Now we examine the scaling of the $m \geq 1$ modes. For $\rho \gg a$, $K_{m\geq 1}(mk_z\rho) \to \frac{1}{\sqrt{2mk_z}} \sqrt{\frac{\pi}{\rho}} e^{-mk_z\rho}$, which means that the typical interaction distance for a dipole is of the order of a from the structure. Inside the MT the modes scale as $\lim_{\rho\to 0} I_m(mk_z\rho) \propto \left(\frac{mk_z\rho}{2}\right)^m$. Importantly, these modes are discrete and are dominated by the $m = 1$ mode for $\rho_0 - \rho_2 \gtrsim a/2$, where ρ_0 is the dipole radius. This means that the response of these modes is highly selective in $\mathbf{k}$. For $\rho_0 - \rho_2 \gtrsim a/2$ the $m = 1$ mode is excited by the dipole and couples to the high-order modes that have a negligible effect at $\rho = \rho_0$ and we can consider approximately only this mode. In Fig. 3 we present the radial dependence of the first modes outside a MT. The modes have a typical interaction distance of the size of $a = 8$nm, which is larger than the Debye distance of 1nm [2], and the $m = 1$ mode dominates at large distances. These functions have m in the radial argument unlike the standard cylindrical modes. Two isopotential surfaces of $\psi_{m=1}(\mathbf{r})$ outside the helical structure are shown in the inset.

To obtain the eigenpermittivities we impose the field boundary conditions (see A.3). We also calculate $\mathbf{E}_{m\geq 1}$ and find that $E_z > E_\rho > E_\phi$, which means that the dipole tends to align almost parallel to the helical structure (see A.4).

The resonances are approached when $\epsilon_{1zk} \approx \epsilon_{1z}(\mathbf{k}, \omega_1)$, where ω_1 is a resonance frequency. Delocalization of modes implies $\text{Im}(\omega_k) \approx 0$ and hence $\text{Re}(\epsilon_{1z}(\mathbf{k}, \omega))$ that spans over a large range of values. Therefore, close to $k = mk_z$ the system is likely to be at a resonance at $\omega_1 \simeq \omega_{k=mk_z}$. When exciting at ω_1 there can be a strong and collective response [43] of the helical structure that may affect the MT functionality. For resonances in additional types of structures see Refs. [44–47]. ϵ_{1zk} depends on the structure dimensions and $\epsilon_{1zk}(\omega)$ on the internal interactions. Hence, ω_1 may enable us to distinguish be-

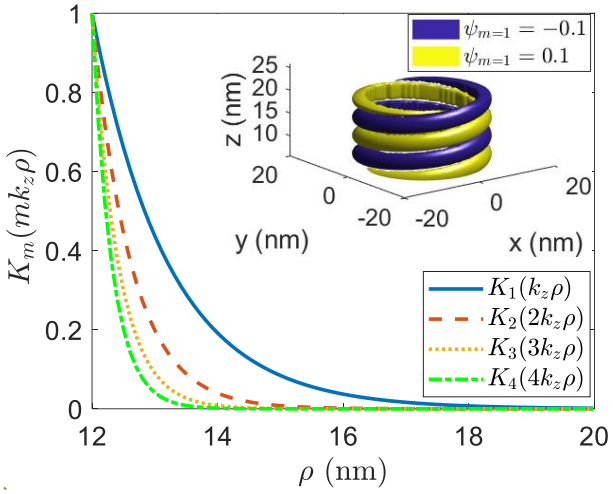

Figure 3: Normalized $K_m(mk_z\rho)$ outside the microtubule. The interaction distance is of the order of a. Inset: two isopotential surfaces of $\psi_{m=1}(\mathbf{r}) = \pm 0.1$ extending to a radius of about 18nm.

tween different helical structures.

The phenomena associated with the helical structure are both in the near and far fields (for $m \geq 1$ and $m = 0$, respectively). They can be observed by absorption spectroscopy [48] with an incoming field polarized along the axial axis [49], by Raman spectroscopy [50], or indirectly, by conductivity measurements [34].

V. SUMMARY

In conclusion, we studied the coupling between EM fields and vibrational-modes in a helical crystal structure by analyzing the bulk and geometric properties of the structure. In particular, we examined the interaction of the structure and oscillating dipole, which emits field components also beyond the first Brillouin zone. We identified a group of discrete modes of in-phase oscillations that give rise to a delocalized response and selectivity in ω and $\mathbf{k}$. We note that in a recent experiment coherent and delocalized response was observed in DNA [33]. We found that the first mode is long-range and scales as $1/\sqrt{\rho}$ while the other modes are quasistatic and have typical interaction distances characterized by the helical-orbit axial period. The fact that the spatial distribution of the $m = 1$ mode correlates with the constituent units may imply spatial selectivity, which can be relevant for processes like self-assembly and induced polymerization. Finally, similar phenomena may arise in other physical systems where the constituent units are self-assembled [51].

Appendix

A.1. The form of the incoming field

When the system size l, which is determined by the inclusion radius and the dipole-inclusion distance, is much smaller than the far-field wavelength λ, $\nabla \times \boldsymbol{E} \approx 0$. Thus, $\boldsymbol{E}$ is decoupled from the magnetic field and can be approximated by Poisson's equation. We consider a two-constituent medium composed of a helical structure, which we regard as the inclusion and a host medium. We then define the incoming field $\boldsymbol{E}_{\rm inc}$ as the dipole field in the host medium. We utilize the expansion of $\boldsymbol{E}_{\rm inc}$ with respect to the structure's axis using cylindrical vector harmonics in order to relate it to the structure's vibrations. A field that is constant along a helical orbit results in synchronous oscillation of laterally-adjacent units. In the case of an axially-periodic structure such as the microtubule, the protofilaments behave as 1D crystals, or in other words, the protafilaments are non-interacting. We impose that $\boldsymbol{E}_{\rm inc}$ is symmetric to a continuous translation along the helical orbit and obtain inside the inclusion volume

$$\begin{aligned}
&\boldsymbol{E}_{{\rm inc},m} \propto e^{im(\phi - k_z z)}, \boldsymbol{E}_{{\rm inc},m} \approx -\nabla\psi_{{\rm inc},m} \\
&\Rightarrow \psi_{{\rm inc},m} \propto e^{im(\phi-k_z z)}, \\
&\nabla_v \psi_{{\rm inc},m} = v \cdot \nabla \psi_{{\rm inc},m} \\
&= -\frac{i}{\sqrt{(\rho k_z)^2+1}} (\rho k_z, 1) \cdot (m/\rho, -m k_z)\, e^{im(\phi-k_z z)} = 0,
\end{aligned}$$

where ϕ, z, ρ are cylindrical coordinates variables, $k_z = 2\pi/a$, and a is the helical-orbit axial period. When the dipole is very close to the helical structure, the field impinging on the microtubule has very high spatial frequencies and it excites additional modes that correspond to coordinated movement and encode the arrangement of the constituent units. These field modes have the relation for the axial index $k = pnk_z$, where p is an integer number and n is the number of units per helical round. Note that this form of the field agrees with the form of a subgroup of terms in a simpler case of the electrostatic potential generated by charges in a helical arrangement in DNA. Our case is much more complex as the inclusion is an anisotropic (and charge-free) medium that is composed of many atoms and we consider excitations of vibrations by electrodynamic field [21].

A.2 Vibrational-mode analysis

A.2.1 Delocalization analysis

The equations of motion (EOM, see Eq. (3) in the manuscript) can be written as

$$\begin{pmatrix} \left[k_1+k_2+4k_3\sin^2\left(\left(ka/n-2\pi m/n\right)/2\right)\right]/m_1 & -\left(k_2e^{-ika}+k_1\right)/m_1 \\ -\left(k_2e^{ika}+k_1\right)/m_2 & \left[k_1+k_2+4k_4\sin^2\left(\left(ka/n-2\pi m/n\right)/2\right)\right]/m_2 \end{pmatrix}\begin{pmatrix} u_1 \\ u_2 \end{pmatrix}=\omega^2\begin{pmatrix} u_1 \\ u_2 \end{pmatrix}.$$

This matrix is Hermitian and therefore diagonalizable and has real eigenvalues. Since the eigenvalue is ω^2 and we are interested that ω will be real, we will prove that the matrix is positive semi-definite so that $\omega_n^2 \geq 0$. For $m_1 = m_2$ we omit the mass and write

$$\begin{pmatrix} u_1^* & u_2^* \end{pmatrix}\begin{pmatrix} \left[k_1+k_2+4k_3\sin^2\left(\left(ka/n-2\pi m/n\right)/2\right)\right] & -\left(k_2e^{-ika}+k_1\right) \\ -\left(k_2e^{ika}+k_1\right) & \left[k_1+k_2+4k_4\sin^2\left(\left(ka/n-2\pi m/n\right)/2\right)\right] \end{pmatrix}\begin{pmatrix} u_1 \\ u_2 \end{pmatrix}$$

$$=\begin{pmatrix} u_1^* & u_2^* \end{pmatrix}\begin{pmatrix} u_1\left[k_1+k_2+4k_3\sin^2\left(\left(ka/n-2\pi m/n\right)/2\right)\right]-u_2\left(k_2e^{-ika}+k_1\right) \\ -u_1\left(k_2e^{ika}+k_1\right)+u_2\left[k_1+k_2+4k_4\sin^2\left(\left(ka/n-2\pi m/n\right)/2\right)\right] \end{pmatrix}$$

$$=k_1\left|u_1-u_2\right|^2+k_2\left|u_1e^{ika}-u_2\right|^2+4\left(k_3\left|u_1\right|^2+k_4\left|u_2\right|^2\right)\sin^2\left(\left(ka/n-2\pi m/n\right)/2\right)\geq 0.$$

This indicates that we can write $\omega(k)$ with real ω or k and therefore the modes are delocalized. We have also verified that $\omega(k)^2 \geq 0$ for $m_1 \neq m_2$ for several values from the analytical solution of Eq. (3) in the manuscript. We consider an external excitation and an excited vibrational mode at ω, k and we therefore need to consider the EOM at these ω, k. When introducing on-site anharmonicity or dissipation, localization can arise since the operator can no longer be written in this form or becomes non-Hermitian. When increasing the dispersion/coupling between u_1 and u_2, it increases the delocalization of the mode [30,31] (these terms are also compatible with Hermiticity). Since the lateral alignment of the units changes upon axial-distance change, it results in different interactions and asymmetric potential (see Fig. A1). We therefore introduce the second-order quadratic force to account for the anharmonicity

$$\begin{aligned} F_1 =& -k_{3\mathrm{an}}\left(u_{1sq}-u_{1s,q+1}\right)^2-k_{3\mathrm{an}}\left(u_{1sq}-u_{1s,q-1}\right)^2 \\ =& -k_{3\mathrm{an}}u_{1sq}^2\left(1-e^{i(ka/n-2\pi m/n)}\right)^2 \\ & -k_{3\mathrm{an}}u_{1sq}^2\left(1-e^{-i(ka/n-2\pi m/n)}\right)^2 \\ =& -2k_{3\mathrm{an}}u_{1sq}^2[1-2\cos\left(ka/n-2\pi m/n\right) \\ & +\cos\left(2\left(ka/n-2\pi m/n\right)\right)]. \end{aligned}$$

This force translates to an on-site anharmonicity and vanishes for the $k = mk_z$ modes. For these modes the $u_1 - u_2$ coupling terms are also maximal. Moving away from these modes increases the ratio of anharmonicity to dispersion, which is associated with localization of modes. The potential now has the same form of the potentials in Refs. 30,31, in which it was shown that phonons become localized when increasing the ratio of the on-site anharmonicity to dispersion/coupling between sites.

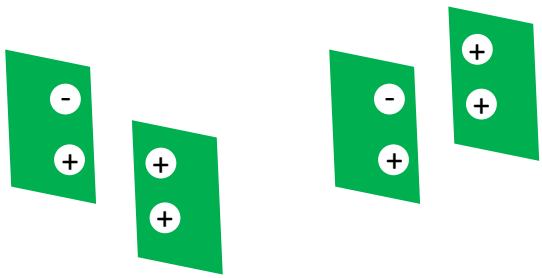

Figure A1: Axial locations of the lateral units in the two states of the right unit, indicating different interactions and anharmonic potential.

A.2.2 Dispersion relation for two helical structures without periodicity and axial interactions

In this section we analyze $\omega(k)$ for helical structures without axial interactions and axial periodicity.

Helix of alternating α, β units without axial interactions

First we analyze $\omega(k)$ for a helix of alternating units without axial interaction (Fig. A2 (a)).

We write the EOM

$$\begin{aligned} -\omega^2 m_1 u_{1sq} &= -k_1\left(u_{1sq}-u_{2s,q+1}\right)-k_1\left(u_{1sq}-u_{2,sq-1}\right), \\ -\omega^2 m_2 u_{2sq} &= -k_1\left(u_{2sq}-u_{1s,q+1}\right)-k_1\left(u_{2sq}-u_{1,sq-1}\right), \end{aligned}$$

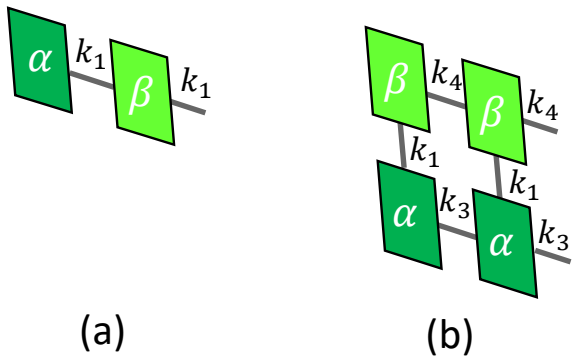

Figure A2: Two helical structures without axial interactions and axial periodicity.

which translate to

$$-\omega^2 m_1 u_{1sq} + 2k_1 \left(u_{1sq} + u_{2sq}\cos\left(ka/n - 2\pi m/n\right)\right) = 0,$$
$$-\omega^2 m_2 u_{2sq} + 2k_1 \left(u_{2sq} + u_{1sq}\cos\left(ka/n - 2\pi m/n\right)\right) = 0,$$

and the matrix form

$$\begin{pmatrix} -\omega^2 m_1 + 2k_1 & 2k_1\cos\left(ka/n - 2\pi m/n\right) \\ 2k_1\cos\left(ka/n - 2\pi m/n\right) & -\omega^2 m_2 + 2k_1 \end{pmatrix} \begin{pmatrix} u_{1sq} \\ u_{2sq} \end{pmatrix} = \begin{pmatrix} 0 \\ 0 \end{pmatrix}.$$

It can be seen that there is strong dispersion in the $k = mk_z$ eigenmodes (associated with delocalization). We write the dispersion relation

$$m_1 m_2 \omega^4 - 2k_1\omega^2\left(m_1 + m_2\right) + 4k_1^2 \sin^2\left(ka/n - 2\pi m/n\right) = 0.$$

From the analogy to a 1D crystal of two particles [24] we observe an in-phase oscillation in the $k = mk_z$ eigenmodes. DNA requires also to introduce a second helix and impose that the sites that interact (base pair) will have the same potential distribution with corresponding modes such as $m = 0, 2$ etc.

Vertical dimers disposed in a helical structure without axial interactions and periodicity

We also consider the model of Fig. 2 in the manuscript without axial interaction between the dimers and without requiring periodicity along the helix (see Fig. A2 (b)). We write the EOM in a matrix

$$\begin{pmatrix} -\omega^2 m_1 + k_1 + 4k_3 \sin^2\left(\left(ka/n - 2\pi m/n\right)/2\right) & -k_1 \\ -k_1 & -\omega^2 m_2 + k_1 + 4k_3 \sin^2\left(\left(ka/n - 2\pi m/n\right)/2\right) \end{pmatrix} \begin{pmatrix} u_{1sq} \\ u_{2sq} \end{pmatrix} = \begin{pmatrix} 0 \\ 0 \end{pmatrix},$$

from which we obtain the dispersion relation for the $k = mk_z$ modes

$$\left(-\omega^2_{k=mk_z} m_1 + k_1\right)\left(-\omega^2_{k=mk_z} m_2 + k_1\right) - k_1^2 = 0,$$
$$\omega^2_{k=mk_z}\left(m_1 m_2 \omega^2_{k=mk_z} - k_1\left(m_1 + m_2\right)\right) = 0,$$
$$\omega^2_{k=mk_z} = k_1\frac{m_1 + m_2}{m_1 m_2}, 0$$

We substitute $\omega^2_{k=mk_z} = k_1\frac{m_1+m_2}{m_1 m_2}$ and get

$$\left(-k_1\frac{m_1 + m_2}{m_1 m_2} m_1 + k_1\right) u_{1sq} - k_1 u_{2sq} = 0,$$
$$-k_1\left(\frac{m_1}{m_2}\right) u_{1sq} - k_1 u_{2sq} = 0,$$
$$u_{2sq} = -\left(\frac{m_1}{m_2}\right) u_{1sq}.$$

Here we see that the $k = mk_z$ modes have the same in-phase oscillations (see video) and behavior associated with the anharmonicity. Note that while in this case the

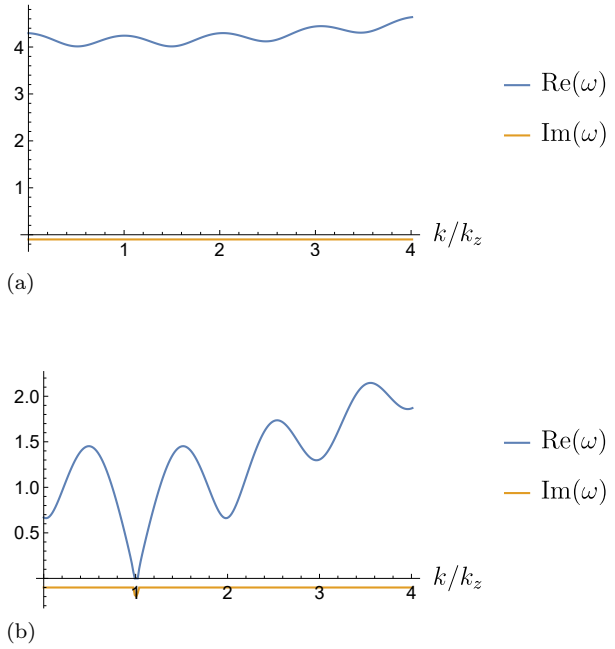

Figure A3: $\omega(k)$ of the optical (a) and acoustical (b) modes for $\gamma = 0.2\,(\mathrm{Kg/s})$

propagation of the vibrations is via the helix, the mathematical structure is similar to Eq. (3) in the manuscript and we can therefore analyze it in the same manner.

A.2.3 Incorporating dissipation to the vibrational-mode analysis

We incorporated dissipation in our model (Fig. 2 (b) in the manuscript) by introducing to Eq. (2) in the manuscript the terms $\gamma\dot{u}_{1,2}$. We first substituted $\gamma = 0$, required that the determinant of the matrix will be equal to zero, and calculated numerically the dispersion relation to verify that it agrees with the analytic calculation. We then calculated numerically $\omega(k)$ for the optical and acoustic modes where $\gamma = 0.2\,(\mathrm{Kg/s})$ and $m_1 = m_2 = 1(\mathrm{Kg})$ for simplicity. By calculating the modes at various γ values we observed that $\mathrm{Re}\left[\omega(k)\right]$ is hardly affected and $\mathrm{Im}\left[\omega(k)\right]$ is constant except at large γ values that suppress the acoustic modes (Fig. A3). This means that, at least for the optical modes, the effect of the dissipation has no preference to a specific k, unlike the effect of the anharmonic terms. In addition, the acoustical modes might be suppressed since $\omega = 0$ there.

A.3 Quasistatic analysis of the interaction between a dipole and helical crystal

A.3.1 Expansion of the potential of a dipole for an anisotropic and spatially-dispersive inclusion

We will start by expanding the physical potential of a charge distribution in a two-constituent medium, in which both constituents are isotropic and spatially uniform, similarly to the treatment in Refs. [15-17]. We will then develop an expansion for an inclusion with an anisotropic and spatially-uniform permittivity and simplify it for a dipole source. Finally, we will formulate the field expansion for a k-dependent inclusion permittivity where the modes are uncoupled and analyze the scattered field for a crystal inclusion.

In the quasistatic regime we use Poisson's equation in a two-constituent medium for the electric potential of a charge distribution $\tilde{\rho}(\mathbf{r})$. When both constituents have a spatially uniform and isotropic permittivities we write [15-17]

$$\nabla\epsilon\nabla\psi = \tilde{\rho}(\mathbf{r}),$$
$$\nabla^2\psi(\mathbf{r}) = \nabla\cdot\theta_1(\mathbf{r})\,u\nabla\psi(\mathbf{r}) + \tilde{\rho}(\mathbf{r})/\epsilon_2, \quad u \equiv \frac{\epsilon_2-\epsilon_1}{\epsilon_2},$$

where $\theta_1(\mathbf{r})$ is a window function that equals 1 inside the inclusion,ϵ_1 is the inclusion permittivity, and ϵ_2 is the host-medium permittivity. The potential can be regarded as generated by the external charge distribution $\tilde{\rho}(\mathbf{r})/\epsilon_2$ and $\nabla\cdot\theta_1(\mathbf{r})\,u\nabla\psi(\mathbf{r})$. Therefore, it can also be expressed as $\psi = \psi_0 + \psi_{\mathrm{sc}}$ in terms of the potential ψ_0 generated by the charge distribution in a uniform ϵ_2 medium (corresponds to $\boldsymbol{E}_{\mathrm{inc}}$ in the manuscript) and ψ_{sc} that is generated due to the existence of the inclusion.

An eigenstate ψ_n, which exists in a system without a source, is defined as follows

$$\nabla^2\psi_n(\mathbf{r}) = \nabla\cdot\theta_1(\mathbf{r})\,u_n\nabla\psi_n(\mathbf{r}), \quad u_n \equiv \frac{\epsilon_2-\epsilon_{1n}}{\epsilon_2},$$
$$\psi_n(\mathbf{r}) = \int G\left(\mathbf{r}-\mathbf{r}'\right)\nabla\cdot\theta_1 u_n\nabla\psi_n\left(\mathbf{r}'\right)d\mathbf{r}'$$
$$= u_n\int\theta_1\left(\mathbf{r}'\right)\nabla G\left(\mathbf{r}-\mathbf{r}'\right)\nabla\psi_n(\mathbf{r}')\,d\mathbf{r}',$$

where $G(\mathbf{r}-\mathbf{r}')$ is Green's function of Poisson's equation and we performed integration by parts. We define the operator $\hat{\Gamma}$as

$$\hat{\Gamma}\psi_n = \int\theta_1\left(\mathbf{r}'\right)\nabla G\left(\mathbf{r}-\mathbf{r}'\right)\nabla\psi_n\left(\mathbf{r}'\right)d\mathbf{r}'$$

and write

$$\psi_n = u_n\hat{\Gamma}\psi_n, \quad s_n\psi_n = \hat{\Gamma}\psi_n, \quad s_n = \frac{1}{u_n}.$$

We then obtain [15-17]

$$\begin{aligned}\psi &= u\hat{\Gamma}\psi + \psi_0 \\ &= \frac{1}{1-u\hat{\Gamma}}\psi_0 = \psi_0 + \frac{u\hat{\Gamma}}{1-u\hat{\Gamma}}\psi_0 \\ &= \psi_0 + \sum_n \frac{u\hat{\Gamma}}{1-u\hat{\Gamma}} |\psi_n\rangle \langle\psi_n|\psi_0\rangle \\ &= \psi_0 + \sum_n \frac{s_n}{s-s_n} |\psi_n\rangle \langle\psi_n|\psi_0\rangle \\ &= \psi_0 + q\sum_n \frac{s_n^2}{s-s_n} |\psi_n\rangle \psi_n^* (\mathbf{r}_0)\end{aligned}$$

where we have used for a point charge [17]

$$\begin{aligned}\langle\psi_n|\psi_0\rangle &= \int d\mathbf{r}\theta_1 \nabla\psi_n^* \nabla\psi_0 \\ &= \int d\mathbf{r}\theta_1 (\mathbf{r}) \nabla\psi_n^* (\mathbf{r}) \nabla \int G(\mathbf{r}-\mathbf{r}') q\delta(\mathbf{r}'-\mathbf{r}_0) d\boldsymbol{r}' \\ &= qs_n \int d\mathbf{r}'\psi_n^* (\mathbf{r}') q\delta(\mathbf{r}'-\mathbf{r}_0) = qs_n\psi_n^* (\mathbf{r}_0).\end{aligned}$$

The eigenstates are assumed to be normalized, where the inner product is defined as

$$\langle\psi_n|\psi_n\rangle = \int d\mathbf{r}\theta_1 \nabla\psi_n^* \nabla\psi_n.$$

Now we develop the expansion of the potential for an anisotropic inclusion permittivity. We denote the inclusion permittivity tensor by $\overleftrightarrow{\epsilon}_1$ and write

$$\begin{aligned}\nabla\overleftrightarrow{\epsilon}\nabla\psi &= \tilde{\rho}(\mathbf{r}), \\ \epsilon_2\nabla^2\psi + \nabla\theta_1 (\overleftrightarrow{\epsilon}_1 - \epsilon_2)\nabla\psi &= \tilde{\rho}(\mathbf{r}), \\ \epsilon_2\nabla^2\psi = \frac{\tilde{\rho}(\mathbf{r})}{\epsilon_2} + \nabla\theta_1 \frac{(\epsilon_2 - \overleftrightarrow{\epsilon}_1)}{\epsilon_2}\nabla\psi, & \\ \nabla^2\psi(\mathbf{r}) = \nabla\cdot\theta_1(\mathbf{r})\overleftrightarrow{u}\nabla\psi(\mathbf{r}) + \frac{\tilde{\rho}(\mathbf{r})}{\epsilon_2}, \quad \overleftrightarrow{u} \equiv \frac{\epsilon_2 I - \overleftrightarrow{\epsilon}_1}{\epsilon_2}.&\end{aligned}$$

where I is the unit matrix.

We define an eigenfunction $\psi_k$as follows

$$\begin{aligned}\psi_k(\mathbf{r}) &= \int G\left(\mathbf{r}-\mathbf{r}'\right)\nabla\cdot\theta_1\overleftrightarrow{u}\nabla\psi_k(\mathbf{r}')d\mathbf{r}' \\ &= \int G\left(\mathbf{r}-\mathbf{r}'\right)\frac{\partial}{\partial' i}\theta_1 u_{k,ij}\frac{\partial}{\partial' j}\psi_k(\mathbf{r}')d\mathbf{r}' \\ &= \sum_{i,j} u_{ij,k} G\left(\mathbf{r}-\mathbf{r}'\right)\frac{\partial}{\partial'_i}\theta_1(\boldsymbol{r}')\frac{\partial}{\partial'_j}\psi_k(\mathbf{r}')d\mathbf{r}' \\ &= \sum_{i,j} u_{ij,k}\theta_1(\boldsymbol{r}')\frac{\partial}{\partial'_i} G\left(\mathbf{r}-\mathbf{r}'\right)\frac{\partial}{\partial'_j}\psi_k(\mathbf{r}')d\mathbf{r}',\end{aligned}$$

where we performed integration by parts and $u_{ij} \equiv \delta_{ij} - \frac{\epsilon_{1ij}}{\epsilon_2}$.

For a diagonal form of $\overleftrightarrow{\epsilon}$ we have

$$\begin{aligned}\psi_k(\mathbf{r}) &= u_{i,k}\int G(\mathbf{r}-\mathbf{r}')\frac{\partial}{\partial'_i}\theta_1(\mathbf{r}')\frac{\partial}{\partial'_i}\psi_k(\mathbf{r}')d\mathbf{r}' \\ &= \sum_i u_{i,k}\int\theta_1(\mathbf{r}')\frac{\partial}{\partial'_i}G(\mathbf{r}-\mathbf{r}')\frac{\partial}{\partial'_i}\psi_k(\mathbf{r}')d\mathbf{r}'.\end{aligned}$$

For $(\epsilon_x,\epsilon_y,\epsilon_z) = (\epsilon_2,\epsilon_2,\epsilon_{1z})$

$$\begin{aligned}\psi_k(\mathbf{r}) &= u_{zk}\int G\left(\mathbf{r}-\mathbf{r}'\right)\frac{\partial}{\partial'_z}\theta_1\left(\mathbf{r}'\right)\frac{\partial}{\partial'_z}\psi_k\left(\mathbf{r}'\right)d\mathbf{r}' \\ &= u_{zk}\int\theta_1\left(\mathbf{r}'\right)\frac{\partial}{\partial'_z}G\left(\mathbf{r}-\mathbf{r}'\right)\frac{\partial}{\partial'_z}\psi_k\left(\mathbf{r}'\right)d\mathbf{r}'.\end{aligned}$$

We write the eigenvalue equation

$$\begin{aligned}\psi_k = u_{zk}\hat{\Gamma}_z\psi_k, \;\; s_{zk}\psi_k = \hat{\Gamma}_z\psi_k, \\ s_{zk} = 1/u_{zk} = \epsilon_2/(\epsilon_2 - \epsilon_{1zk}),\end{aligned}$$

where s_{zk} is an eigenvalue. Note that here the physical permittivity of the inclusion ϵ_1 is spatially uniform and the index k denotes the mode index. Similarly, we write the expansion of ψ for $(\epsilon_x,\epsilon_y,\epsilon_z) = (\epsilon_x,\epsilon_y,\epsilon_{1z})$

$$\psi = \psi_0 + \sum_k \frac{s_{zk}}{s_z - s_{zk}} |\psi_n\rangle \langle\psi_n|\psi_0\rangle$$

For a point charge we substitute the eigenvalue equation in the inner product to obtain

$$\begin{aligned}\langle\psi_k|\psi_0\rangle &= \int d\mathbf{r}\theta_1(\mathbf{r})\frac{\partial}{\partial z}\psi_k^*(\mathbf{r})\frac{\partial}{\partial z}\psi_0(\mathbf{r}) \\ &= \frac{4\pi}{\epsilon_2}\int d\mathbf{r}\theta_1(\mathbf{r})\frac{\partial}{\partial z}\psi_k^*(\mathbf{r})\frac{\partial}{\partial z}G\left(\mathbf{r}-\mathbf{r}'\right) * q\delta\left(\mathbf{r}'-\mathbf{r}_0\right) \\ &= \frac{4\pi q}{\epsilon_2}s_{zk}\psi_k^*(\mathbf{r}_0).\end{aligned}$$

We then consider a dipole composed of two charges and write

$$\begin{aligned}\langle\psi_k|\psi_0\rangle &= s_{zk}q\left(\psi_k^*(\mathbf{z}_0 + \mathbf{d}/2) - \psi_k^*(\mathbf{z}_0 - \mathbf{d}/2)\right) \\ &= s_{zk}qd\frac{(\psi_k^*(\mathbf{z}_0 + \mathbf{d}/2) - \psi_k^*(\mathbf{z}_0 - \mathbf{d}/2))}{d}.\end{aligned}$$

For a cylindrical inclusion, the eigenfunctions have two indices m,k. All in all, we obtain for ψ

$$\psi = \psi + \frac{4\pi}{\epsilon_2}\sum_m\int\frac{s_k^2}{s_z - s_k}|\psi_{m,k}\rangle\nabla\psi_{m,k}^*(\mathbf{r}_0)\cdot\mathbf{p}dk, \tag{A.1}$$

where the inner product for the normalization is

$$\langle\psi_k|\psi_k\rangle = \int d\mathbf{r}\theta_1(\mathbf{r})\frac{\partial}{\partial z}\psi_{m,k}^*(\mathbf{r})\frac{\partial}{\partial z}\psi_{m,k}(\mathbf{r}).$$

We now formulate the expansion for a k-dependent inclusion permittivity without coupling between modes. This is the situation in an electron gas, where the physical permittivity value is associated with each mode [24]. We

first write the response of the inclusion to an excitation at a given k

$$\psi_{\mathrm{sc},k} = \frac{u_{zk}\Gamma_z}{1-u_{zk}\Gamma_z}\psi_{0k},$$

where u_{zk} corresponds to the physical inclusion permittivity at a given k and

$$\psi_{0k} = \langle\psi_0|\psi_k\rangle\,\psi_k.$$

We can now sum these terms and substitute in Eq. (A.1) $s_z \to s_z(m,k)$ to obtain for a cylindrical inclusion

$$\psi = \psi_0 + \frac{4\pi}{\epsilon_2}\sum_m \int \frac{s_{km}^2}{s_z(m,k)-s_{km}} |\psi_{km}\rangle \nabla\psi_{km}^*(\mathbf{r}_0)\cdot\mathbf{p}dk. \quad . \tag{A.2}$$

Finally, we analyze the response of a crystal inclusion. In the case of a helical crystal the Fourier expansion is along a helical orbit and the "DC" components have constant potential along this orbit. We thus have coupling between modes of the types [25] $(m',k') \to \left(m'+pm, k'+pmk_z\right)$ and $(m',k') \to \left(m', k'+pnk_z\right)$, where p is an integer number and n is the number of units per helical round. We will show in the next subsection that for $\rho_0-\rho_2 > a/n$, $\rho_0-\rho_2 > a/2$ the second and first types of coupling are negligible, respectively, at $\rho=\rho_0$. We therefore conclude that for $\rho_0-\rho_2 > a/2$ only the $m=1$ mode is important and write

$$\psi(\boldsymbol{r}, \rho_0 > a/2) \approx$$
$$\psi_0(\boldsymbol{r}) + \frac{4\pi}{\epsilon_2}\int \frac{s_{km=1}^2}{s_z(m=1,k)-s_{km=1}} |\psi_{km}\rangle \nabla\psi_{km}^*(\mathbf{r}_0)\cdot\mathbf{p}dk \tag{A.3}$$

We can substitute the eigenpermittivities and the physical permittivity, to get $s_z(m=1,k), s_{k,m=1}$, respectively, and obtain an expansion for $\psi(\mathbf{r})$. The calculation of the eigenpermittivities will be explained in this section and the physical permittivity can be measured in some cases or calculated by substituting $\omega(k) \to \omega_T$ in the expression for ϵ [23]. $\omega(k)$ is calculated in the manuscript from the EOM and can also be calculated when anharmonic terms are incorporated (see references in Ref. 30).

Since a strong response is expected at $m=1, k=k_z$ (see explanation in the manuscript in pages 4-5), a dipole that emits at a range of spatial frequencies will interact more dominantly with this mode. In this region the dominant term in the expansion is

$$\frac{4\pi}{\epsilon_2}\frac{s_{k_zm=1}^2}{s_z(m=1,k_z)-s_{k_zm=1}} |\psi_{k_zm=1}\rangle \nabla\psi_{k_zm=1}^*(\mathbf{r}_0)\cdot\mathbf{p},$$

in addition to ψ_0, where $k_z = \frac{2\pi}{a}$, a is the helical-orbit axial periodicity.

Finally, ψ_0 can also be expanded by a set of eigenfunctions inside the inclusion as follows

$$\psi_0 = \sum_m \int dk\,\langle\psi_0|\psi_{km}\rangle\,\langle\psi_{km}|$$
$$= \sum_m s_{mk}\int |\psi_{km}\rangle \nabla\psi_{km}^*(\mathbf{r}_0)\cdot\mathbf{p}dk.$$

A.3.2 The form of the eigenfunctions

Since $\boldsymbol{E}_{\mathrm{inc}}/\psi_0$ component with a given k results in a contribution of an eigenfunction with the same k in the expansion, the eigenfunctions that account for the field scattering due to synchronous vibrations are

$$\psi_m = e^{im(\phi-k_zz)}\begin{cases} A_{1m}K_m(mk_z\rho) & \rho>\rho_2 \\ A_{2m}I_m + A_{3m}K_m & \rho_1<\rho<\rho_2 \\ A_{4m}I_m(mk_z\rho) & \rho<\rho_1 \end{cases},$$

where ϕ, z, ρ are cylindrical coordinates variables, I_m, K_m are the modified Bessel functions, ρ_1, ρ_2 are the internal and external inclusion radii, $k_z = 2\pi/a$, and a is the helical-orbit axial period. Upon a continuous translation along the helical orbit, ψ_m remains constant and therefore corresponds to an eigenvalue 1. We can similarly take the directional derivative in the direction of the helical orbit and obtain

$$\nabla_v\psi_m = v\cdot\nabla\psi_m$$
$$= -\frac{i}{\sqrt{(\rho k_z)^2+1}}(\rho k_z, 1)\cdot(m/\rho, -mk_z)\,e^{im(\phi-k_zz)} = 0,$$

as expected. This means that $\hat{R}\psi_n = \psi_n$, where $\hat{R}$ is the continuous-translation operator.

A.3.3 Scaling of the eigenfunctions

We analyze the scaling of ψ_m for small and large ρs. We start with the first $m=0$ mode

$$K_m(x\to 0) \to \begin{cases} -\left[\ln\left(\frac{x}{2}\right)+0.5772\right] & m=0 \\ \frac{\Gamma(m)}{2}\left(\frac{2}{x}\right)^m & m\neq 0 \end{cases}$$

Since for $m=0, x=0$ and we expect a finite potential, this mode is associated in all regions with $I_{m=0}(x)$ and is constant everywhere (and therefore can be omitted). This mode can be treated in the full Maxwell-equation analysis and can be shown to scale as $\sqrt{1/\rho}$ [22]. We proceed to the $m\geq 1$ modes at $\rho \gg a$ and obtain

$$K_{m\geq 1}(\rho \gg a) \to \frac{1}{\sqrt{2mk_z}}\sqrt{\frac{\pi}{\rho}}e^{-mk_z\rho},$$

with a typical interaction distance on the order of a/m. This determines the range in which a dipole interacts with each mode.

The scaling of the helical modes inside the structure is

$$I_m(x\to 0)\to \frac{1}{\Gamma(m+1)}\left(\frac{x}{2}\right)^m,$$
$$I_{m=0}(mk_z\rho\to 0)\to \frac{1}{\Gamma(m+1)}\left(\frac{mk_z\rho}{2}\right)^m$$
$$=m^m\left(\frac{k_z\rho}{2}\right)^m,\ \ \Gamma(m+1)=m!.$$

A.3.4 Calculating the radial argument inside the inclusion

In a crystal one can write the effective permittivity $\epsilon=\epsilon(\omega,k)$, which relates the response at a given k to an excitation at the same k. In the case of a microtubule (MT), this form of $\epsilon(\omega,k)$ is justified because the period length a is 8nm and therefore, $(\lambda_0/a)^2\gg 1$ where $\lambda_0=c/\omega$ is the vacuum wavelength [25]. Note that in the derivation in Ref. [25] it is assumed that inside the inclusion $\rho_{\text{ext}}(\omega)=0, \boldsymbol{J}_{\text{ext}}(\omega)=0$, which is satisfied in our case since the charges on the tubulin and tubulin dimers oscillate only as a response to an external excitation and can therefore be defined as polarization. Also, eigenstates are defined for the system without a source. Another argument is that for sources at distances larger than the typical interaction distance of the $m=2$ mode, the inclusion is not affected by the $m>1$ modes.

To represent axial vibrations, we assume an anisotropic inclusion with an axial permittivity ϵ_z and radial and azimuthal permittivitties ϵ_2, equal to the host-medium permittivity, where we omit k for brevity. Note that the eigenpermittivities in the quasistatic regime do not depend on ω. We now solve Laplace's equation in cylindrical coordinates inside the anisotropic inclusion. This will allow us to find the argument of the functions I_m, K_m for $\rho_1<\rho<\rho_2$ and calculate the eigenpermittivities in the next subsection. Substituting the form of ψ_m we write Laplace's equation inside the helical structure

$$\nabla\overleftrightarrow{\epsilon}\nabla\psi_m=0,$$

$$\epsilon_2\frac{1}{\rho}\frac{\partial}{\partial\rho}\left(\rho\frac{\partial\psi_m}{\partial\rho}\right)-\epsilon_2 m^2\frac{1}{\rho^2}\psi_m-k_z^2m^2\epsilon_{zm}\psi_m=0.$$

We change variables

$$x\equiv km\sqrt{\epsilon_z/\epsilon_2}\rho,\ \ \frac{\partial}{\partial\rho}=\frac{\partial}{\partial x}\frac{\partial x}{\partial\rho}=\frac{\partial}{\partial x}k_zm\sqrt{\epsilon_{zm}/\epsilon_2},$$

and write

$$\frac{1}{x}k_z^2m^2\epsilon_{zm}\frac{\partial}{\partial x}\left(x\frac{\partial\psi_m}{\partial x}\right)-m^2\frac{\left(k_zm\sqrt{\epsilon_{zm}}\right)^2}{x^2}\psi_m-k_z^2m^2\epsilon_{zm}\psi_m=0,$$

$$\frac{1}{x}\frac{\partial}{\partial x}\left(x\frac{\partial\psi_m}{\partial x}\right)-\left(\frac{m^2}{x^2}\psi_m+1\right)\psi_m=0,$$

Thus we get

$$\psi_m=e^{im(\phi-k_zz)}\begin{cases}A_{1m}K_m(mk_z\rho) & \rho>\rho_2\\ A_{2m}I_m\left(mk_z\sqrt{\frac{\epsilon_{zm}}{\epsilon_2}}\rho\right)+A_{3m}K_m\left(mk_z\sqrt{\frac{\epsilon_{zm}}{\epsilon_2}}\rho\right) & \rho_1<\rho<\rho_2\\ A_{4m}I_m(mk_z\rho) & \rho<\rho_1\end{cases},$$

which needs to be multiplied by additional factors to obtain the contribution in the expansion of the potential of a point charge as we showed in the previous subsection.

In the more general case of diagonal permittivity $\epsilon=(\epsilon_\rho,\epsilon_\phi,\epsilon_z)$ we write

$$\frac{\epsilon_\rho}{\epsilon_z}\frac{1}{\rho}\frac{\partial}{\partial\rho}\left(\rho\frac{\partial\psi_m}{\partial\rho}\right)-\frac{\epsilon_\phi}{\epsilon_z}m^2\frac{1}{\rho^2}\psi_m-k_z^2m^2\psi_m=0.$$

We change variables

$$x\equiv k_zm\sqrt{\epsilon_z/\epsilon_\rho}\rho,\ \ \frac{\partial}{\partial\rho}=\frac{\partial}{\partial x}\frac{\partial x}{\partial\rho}=\frac{\partial}{\partial x}k_zm\sqrt{\epsilon_z/\epsilon_\rho},$$

and get

$$\frac{1}{x}\frac{\partial}{\partial x}\left(x\frac{\partial\psi_m}{\partial x}\right)-\frac{\epsilon_\phi}{\epsilon_\rho}\frac{m^2}{x^2}\psi_m-\psi_m=0,$$

from which we obtain $v=m\sqrt{\frac{\epsilon_\phi}{\epsilon_\rho}}$

$$\psi_m=e^{im(\phi-k_z z)}\begin{cases}A_{1m}K_m\left(mk_z\rho\right) & \rho>\rho_2\\ A_{2m}I_v\left(mk_z\sqrt{\frac{\epsilon_{zm}}{\epsilon_\rho}}\rho\right)+A_{3m}K_v\left(mk_z\sqrt{\frac{\epsilon_{zm}}{\epsilon_\rho}}\rho\right) & \rho_1<\rho<\rho_2\\ A_{4m}I_m\left(mk_z\rho\right) & \rho<\rho_1\end{cases}.$$

A.3.5 Calculating the eigenpermittivities

We express the eigenvalue equation and the relation between the coefficients, where B_1 is treated as known (cancels out in the expansion). We first write the boundary conditions

$$\begin{aligned}Aa&=B_1b_{11}+B_2b_{21},\\ B_1b_{12}+B_2b_{22}&=C_1c,\\ Aa_d&=\left(B_1b_{11d}+B_2b_{21d}\right),\\ \left(B_1b_{12d}+B_2b_{22d}\right)&=C_1c_d,\end{aligned}$$

where $A\leftrightarrow A_{1mk}, B_1\leftrightarrow A_{2mk}, B_2\leftrightarrow A_{3mk}, C_1\leftrightarrow A_{4mk}$, and

$$a=I_m\left(mk_z\rho_1\right), b_{11}^{\pm}=I_m\left(mk_z\sqrt{\frac{\epsilon_{1m}^{\pm}}{\epsilon_2}}\rho_1\right), b_{12}^{\pm}=I_m\left(mk_z\sqrt{\frac{\epsilon_{1m}^{\pm}}{\epsilon_2}}\rho_2\right),\ b_{21}^{\pm}=K_m\left(mk_z\sqrt{\frac{\epsilon_{1m}^{\pm}}{\epsilon_2}}\rho_1\right),$$

$$b_{22}^{\pm}=K_m\left(mk_z\sqrt{\frac{\epsilon_{1m}^{\pm}}{\epsilon_2}}\rho_2\right),\ c=K_m\left(mk_z\rho_2\right),\ a_d=\left(\frac{\partial I_m\left(mk_z\rho\right)}{\partial\rho}\right)_{\rho=\rho_1},$$

$$b_{11d}^{\pm}=\left(\frac{\partial}{\partial\rho}I_m\left(mk_z\sqrt{\frac{\epsilon_{1m}^{\pm}}{\epsilon_2}}\rho\right)\right)_{\rho=\rho_1}, b_{12d}^{\pm}=\left(\frac{\partial}{\partial\rho}I_m\left(mk_z\sqrt{\frac{\epsilon_{1m}^{\pm}}{\epsilon_2}}\rho\right)\right)_{\rho=\rho_2},$$

$$b_{21d}^{\pm}=\left(\frac{\partial}{\partial\rho}K_m\left(mk_z\sqrt{\frac{\epsilon_{1m}^{\pm}}{\epsilon_2}}\rho\right)\right)_{\rho=\rho_1}, b_{22d}^{\pm}=\left(\frac{\partial}{\partial\rho}K_m\left(mk_z\sqrt{\frac{\epsilon_{1m}^{\pm}}{\epsilon_2}}\rho\right)\right)_{\rho=\rho_2},\ c_d=\left(\frac{\partial K_m\left(mk_z\rho\right)}{\partial\rho}\right)_{\rho=\rho_2}.$$

We write two relations between B_2 and ϵ_{1m}

$$\left(B_1b_{12d}+B_2b_{22d}\right)=\frac{B_1b_{12}+B_2b_{22}}{c}c_d, \qquad (A.4)$$

$$\frac{B_1b_{11}+B_2b_{21}}{a}a_d=\left(B_1b_{11d}+B_2B_{21d}\right), \qquad (A.5)$$

From Eq. (A.4) we express B_2

$$B_2b_{22d}-\frac{B_2b_{22}c_d}{c}=\frac{B_1b_{12}}{c}c_d-B_1b_{12d},$$

$$B_2\left(b_{22d}-\frac{b_{22}c_d}{c}\right)=B_1\left(\frac{b_{12}}{c}c_d-b_{12d}\right),$$

$$B_2 = B_1 \left(\frac{\frac{b_{12}}{c} c_d - b_{12d}}{b_{22d} - \frac{b_{22} c_d}{c}} \right).$$

Substituting this expression in Eq. (5) we obtain the eigenvalue equation for ϵ_{1m}

$$\frac{B_1 b_{11} + B_1 \left(\frac{\frac{b_{12}}{c} c_d - b_{12d}}{b_{22d} - \frac{b_{22} c_d}{c}} \right) b_{21}}{a} a_d = \left(B_1 b_{11d} + B_1 \left(\frac{\frac{b_{12}}{c} c_d - b_{12d}}{b_{22d} - \frac{b_{22} c_d}{c}} \right) b_{21d} \right),$$

$$\left[b_{11} + \left(\frac{\frac{b_{12}}{c} c_d - b_{12d}}{b_{22d} - \frac{b_{22} c_d}{c}} \right) b_{21} \right] \frac{a_d}{a} = \left(b_{11d} + \left(\frac{\frac{b_{12}}{c} c_d - b_{12d}}{b_{22d} - \frac{b_{22} c_d}{c}} \right) b_{21d} \right),$$

$$\left[b_{11} \left(b_{22d} - \frac{b_{22} c_d}{c} \right) + \left(\frac{b_{12}}{c} c_d - b_{12d} \right) b_{21} \right] \frac{a_d}{a} = \left(b_{11d} \left(b_{22d} - \frac{b_{22} c_d}{c} \right) + \left(\frac{b_{12}}{c} c_d - b_{12d} \right) b_{21d} \right),$$

$$0 = \left(b_{22d} - \frac{b_{22} c_d}{c} \right) \left(b_{11d} - b_{11} \frac{a_d}{a} \right) + \left(\frac{b_{12}}{c} c_d - b_{12d} \right) \left(b_{21d} - b_{21} \frac{a_d}{a} \right).$$

Using this equation we can calculate ϵ_{1m}. We calculated numerically ϵ_{1m} for the first modes. Interestingly, due to the anisotropy there is an infinite degeneracy in the quasistatic (real) eigenvalues and each mode has an infinite number of eigenpermittivities, similarly to electrodynamics.

Finally, we express A and C_1

$$A = B_1 \frac{b_{11} + \left(\frac{\frac{b_{12}}{c} c_d - b_{12d}}{b_{22d} - \frac{b_{22} c_d}{c}} \right) b_{21}}{a},$$

$$C_1 = B_1 \frac{b_{12} + \left(\frac{\frac{b_{12}}{c} c_d - b_{12d}}{b_{22d} - \frac{b_{22} c_d}{c}} \right) b_{22}}{c}.$$

A.3.6 Calculating the inner product

We calculate the inner product for completeness. Since the integration over the z, ϕ degrees of freedoms is trivial we focus on the integration with respect to ρ

$$\langle \psi_n | \psi_n \rangle \propto$$

$$\int \left(B_1 I_1 (b\rho) + B_2 K_1 (b\rho) \right)^* \cdot \left(B_1 I_1 (b\rho) + B_2 K_1 (b\rho) \right) d\rho,$$

where $b = \sqrt{\frac{\epsilon_{1zk}}{\epsilon_2}} k$.

We calculate $\langle \psi_n | \psi_n \rangle$ for $b = i\sqrt{\frac{|\epsilon_{1zk}|}{\epsilon_2}} k$

$$\int \left(B_1 I_1 (b\rho) + B_2 K_1 (b\rho) \right)^* \cdot \left(B_1 I_1 (b\rho) + B_2 K_1 (b\rho) \right) d\rho =$$

$$\int |B_1|^2 |I_1 (b\rho)|^2 + |B_2|^2 |K_1 (b\rho)|^2$$

$$+ B_1^* I_1^* (b\rho) B_2 K_1 (b\rho) + B_2^* K_1^* (b\rho) B_1 I_1 (b\rho) \, d\rho.$$

We use the identities

$$I_m (ix) = i^{-m} J_m (-x) = i^{-m} (-1)^m J_m (x),$$

$$I_1 (ix) = i J_m (x),$$

$$K_m (ix) = \frac{\pi}{2} i^{m+1} H_m^{(1)} (-x), \;\; K_1 (ix) = \frac{\pi}{2} (-1) H_1^{(1)} (-x),$$

to simplify the first and second term and obtain

$$\int |B_1|^2 |I_1 (b\rho)|^2 = \int |B_1|^2 J_1 (|b| \rho)^2 \, d\rho,$$

$$\int |B_2|^2 |K_1 (b\rho)|^2 = \left(\frac{\pi}{2} \right)^2 |B_2|^2 \int \left(J (|b| \rho)^2 + Y^2 (|b| \rho) \right) d\rho.$$

We simplify the third and fourth terms by summing the values of two adjacent ρ values

$$B_1^* I_1^* \left(b\rho_1'\right) B_2 K_1 \left(b\rho_1'\right) + B_2^* K_1^* \left(b\rho_1'\right) B_1 I_1 \left(b\rho_1'\right) + B_1^* I_1^* \left(b\rho_2'\right) B_2 K_1 \left(b\rho_2'\right) + B_2^* K_1^* \left(b\rho_2'\right) B_1 I_1 \left(b\rho_2'\right)$$

$$2\mathrm{Re}\left(B_1^* I_1^* \left(b\rho_1'\right) B_2 K_1 \left(b\rho_1'\right)\right) + 2\mathrm{Re}\left(B_1^* I_1^* \left(b\rho_2'\right) B_2 K_1 \left(b\rho_2'\right)\right) =$$

$$2\mathrm{Re}\left(B_1^* I_1^* \left(b\rho_1'\right) B_2 K_1 \left(b\rho_1'\right) + B_1^* I_1^* \left(b\rho_2'\right) B_2 K_1 \left(b\rho_2'\right)\right) =$$

$$2\mathrm{Re}\left(B_1^* B_2 I_1^* \left(b\rho_1'\right) K_1 \left(b\rho_1'\right) + B_1^* B_2 I_1^* \left(b\rho_2'\right) K_1 \left(b\rho_2'\right)\right) =$$

$$2\left[\mathrm{Re}\left(B_1^* B_2\right) \mathrm{Re}\left(I_1^* \left(b\rho_1'\right) K_1 \left(b\rho_1'\right)\right) - \mathrm{Im}\left(B_1^* B_2\right) \mathrm{Im}\left(I_1^* \left(b\rho_1'\right) K_1 \left(b\rho_1'\right)\right)\right]$$

$$+2\left[\mathrm{Re}\left(B_1^* B_2\right) \mathrm{Re}\left(I_1^* \left(b\rho_2'\right) K_1 \left(b\rho_2'\right)\right) - \mathrm{Im}\left(B_1^* B_2\right) \mathrm{Im}\left(I_1^* \left(b\rho_2'\right) K_1 \left(b\rho_2'\right)\right)\right] =$$

$$2\mathrm{Re}\left(B_1^* B_2\right) \left(\mathrm{Re}\left(I_1^* \left(b\rho_1'\right) K_1 \left(b\rho_1'\right)\right) + \mathrm{Re}\left(I_1^* \left(b\rho_2'\right) K_1 \left(b\rho_2'\right)\right)\right)$$

$$-2\mathrm{Im}\left(B_1^* B_2\right) \left(\mathrm{Im}\left(I_1^* \left(b\rho_1'\right) K_1 \left(b\rho_1'\right)\right) + \mathrm{Im}\left(I_1^* \left(b\rho_2'\right) K_1 \left(b\rho_2'\right)\right)\right).$$

From this we deduce

$$\int B_1^* I_1^* \left(b\rho\right) B_2 K_1 \left(b\rho\right) + B_2^* K_1^* \left(b\rho\right) B_1 I_1 \left(b\rho\right) d\rho =$$

$$2\mathrm{Re}\left(B_1^* B_2\right) \int \mathrm{Re}\left(I_1^* \left(b\rho\right) K_1 \left(b\rho\right)\right) d\rho - 2\mathrm{Im}\left(B_1^* B_2\right) \int \mathrm{Im}\left(I_1^* \left(b\rho\right) K_1 \left(b\rho\right)\right) d\rho.$$

All in all we get

$$\int \left(B_1 I_1 \left(b\rho\right) + B_2 K_1 \left(b\rho\right)\right)^* \cdot \left(B_1 I_1 \left(b\rho\right) + B_2 K_1 \left(b\rho\right)\right) d\rho =$$

$$\int \left|B_1\right|^2 J_1 \left(\left|b\right| \rho\right)^2 d\rho + \frac{\pi}{2} \left|B_2\right|^2 \int \left(J \left(\left|b\right| \rho\right)^2 + Y^2 \left(\left|b\right| \rho\right)\right) d\rho$$

$$+\mathrm{Re}\left(B_1^* B_2\right) \int \pi J \left(\left|b\right| \rho\right) Y \left(\left|b\right| \rho\right) d\rho - \mathrm{Im}\left(B_1^* B_2\right) \int \pi J_1^2 \left(\left|b\right| \rho\right) d\rho =$$

$$\int \left|B_1\right|^2 J_1 \left(\left|b\right| \rho\right)^2 d\rho + \left(\frac{\pi}{2}\right)^2 \left|B_1\right|^2 \left|B_{1\to 2}\right|^2 \int \left(J \left(\left|b\right| \rho\right)^2 + Y^2 \left(\left|b\right| \rho\right)\right) d\rho$$

$$+ \left|B_1\right|^2 \left[\mathrm{Re}\left(B_{1\to 2}\right) \int \pi J \left(\left|b\right| \rho\right) Y \left(\left|b\right| \rho\right) d\rho - \mathrm{Im}\left(B_1^* B_2\right) \int \pi J_1^2 \left(\left|b\right| \rho\right) d\rho\right].$$

We calculate the integrals analytically

$$\int J_1 \left(k \left|\sqrt{\frac{\epsilon_{1m}}{\epsilon_2}}\right| \rho\right)^2 = \frac{1}{2} \rho^2 \left(J_m \left(k \left|\sqrt{\frac{\epsilon_{1m}}{\epsilon_2}}\right| \rho\right)^2 - J_{m-1} \left(k \left|\sqrt{\frac{\epsilon_{1m}}{\epsilon_2}}\right| \rho\right) J_{m+1} \left(k \left|\sqrt{\frac{\epsilon_{1m}}{\epsilon_2}}\right| \rho\right)\right),$$

$$\left(\frac{\pi}{2}\right)^2 \left|B_{1\to 2}\right|^2 \int \left(J \left(\left|b\right| \rho\right)^2 + Y^2 \left(\left|b\right| \rho\right)\right) d\rho =$$

$$\frac{1}{4}\pi^2 \left|B_{1\to 2}\right|^2 \left[\frac{1}{2}\rho^2 \left(J_m^2\left(k\left|\sqrt{\frac{\epsilon_{1m}}{\epsilon_2}}\right|\rho\right) - J_{m-1}\left(k\left|\sqrt{\frac{\epsilon_{1m}}{\epsilon_2}}\right|\rho\right) J_{m+1}\left(k\left|\sqrt{\frac{\epsilon_{1m}}{\epsilon_2}}\right|\rho\right)\right)\right.$$

$$\left. +\frac{1}{2}\rho^2 \left(Y_m^2\left(k\left|\sqrt{\frac{\epsilon_{1m}}{\epsilon_2}}\right|\rho\right) - Y_{m-1}\left(k\left|\sqrt{\frac{\epsilon_{1m}}{\epsilon_2}}\right|\rho\right) Y_{m+1}\left(k\left|\sqrt{\frac{\epsilon_{1m}}{\epsilon_2}}\right|\rho\right)\right)\right],$$

$$\mathrm{Re}\left(B_{1\to 2}\right)\int \pi J\left(k\left|\sqrt{\frac{\epsilon_{1m}}{\epsilon_2}}\right|\rho\right) Y\left(k\left|\sqrt{\frac{\epsilon_{1m}}{\epsilon_2}}\right|\rho\right) d\rho - \mathrm{Im}\left(B_1^* B_2\right)\int \pi J_1^2\left(k\left|\sqrt{\frac{\epsilon_{1m}}{\epsilon_2}}\right|\rho\right) d\rho =$$

$$\frac{\pi \mathrm{Re}\left(B_{1\to 2}\right)\left(\frac{2m^2 \csc(\pi m)\Gamma(m+1)\left(-1+{}_2F_2\left(-\frac{1}{2};-m,m;-k^2\rho^2\left|\frac{\epsilon_{1m}}{\epsilon_2}\right|\right)-1\right)}{k^2\left|\frac{\epsilon_{1m}}{\epsilon_2}\right|\Gamma(1-m)} + \frac{4^{-m}\rho^2\cot(\pi m)\left|\frac{\epsilon_{1m}}{\epsilon_2}\right|^m (k\rho)^{2m}\, {}_2F_2\left(m+\frac{1}{2};m+2,2m+1;-k^2\rho^2\left|\frac{\epsilon_{1m}}{\epsilon_2}\right|\right)}{m+1}\right)}{2\Gamma\left(m+1\right)^2}$$

$$-\frac{\pi}{2}\rho^2 \mathrm{Im}\left(B_{1\to 2}\right)\left(J_m\left(k\left|\sqrt{\frac{\epsilon_{1m}}{\epsilon_2}}\right|\rho\right)^2 - J_{m-1}\left(k\left|\sqrt{\frac{\epsilon_{1m}}{\epsilon_2}}\right|\rho\right) J_{m+1}\left(k\left|\sqrt{\frac{\epsilon_{1m}}{\epsilon_2}}\right|\rho\right)\right),$$

where F is a hypergeometric function. All the analytical calculations have been verified with numerical calculations.

A.4 Calculating the electric field of ψ_m

To calculate $\mathbf{E}_{m\geq 1}$ we use

$$\frac{\partial}{\partial\rho}K_m\left(k_z m\rho\right) = -\frac{1}{2}k_z m\left(K_{m-1}\left(k_z m\rho\right) + K_{m+1}\left(k_z m\rho\right)\right),$$

and write, assuming $\psi_m \propto \cos\left(m\left(\phi - k_z z\right)\right)$

$$\mathbf{E}_{m\geq 1} = C_m\left[\frac{1}{2}k_z m\left(K_{m-1}\left(k_z m\rho\right) + K_{m+1}\left(k_z m\rho\right)\right)\cos\left(m\left(\phi - k_z z\right)\right)\mathbf{e}_\rho + \left(\frac{m}{\rho}\mathbf{e}_\phi - k_z\mathbf{e}_z\right)K_m\left(k_z m\rho\right)\sin\left(m\left(\phi - k_z z\right)\right)\right],$$

where C_m is the expansion coefficient. For $m = 1$ we have

$$\mathbf{E}_{m=1} = C_{m=1p}\left[\frac{1}{2}k_z\left(K_0\left(k_z\rho\right) + K_2\left(k_z\rho\right)\right)\cos\left(\phi - k_z z\right)\mathbf{e}_\rho + \left(\frac{1}{\rho}\mathbf{e}_\phi - k_z\mathbf{e}_z\right)K_1\left(k_z\rho\right)\sin\left(\phi - k_z z\right)\right],$$

$$C_{m=1p} \propto \mathbf{p}\cdot\left[\frac{1}{2}k_z\left(K_0\left(k_z\rho\right) + K_2\left(k_z\rho\right)\right)\cos\left(\phi - k_z z\right)\mathbf{e}_\rho + \left(\frac{1}{\rho}\mathbf{e}_\phi - k_z\mathbf{e}_z\right)K_1\left(k_z\rho\right)\sin\left(\phi - k_z z\right)\right].$$

[1] A. Mershin, A. A. Kolomenski, H. Schuessler, and D. V. Nanopoulos Tubulin dipole moment, dielectric constant and quantum behavior: computer simulations, experimental results and suggestions. Biosystems **77**, 73 (2004).

[2] J. Preto, M. Pettini, and J. A. Tuszynski, Possible role of electrodynamic interactions in long-distance biomolecular recognition. Phys. Rev. E **91**, 052710 (2015).

[3] J. A Tuszynski, T. Luchko, E. J. Carpenter, and E. Crawford, Results of molecular dynamics computations of the structural and electrostatic properties of tubulin and their consequences for microtubules. Journal of Computational and Theoretical Nanoscience **1**, 4 (2004).

[4] R. Guzman, R. Wu, Aarat P. Kalra, M. Aminpour, J.A. Tuszynski, and A. Dogariu, Tubulin polarizability in aqueous suspensions. ACS Omega **4**, 9144 (2019).

[5] J. Tuszynski, C. Wenger, D. Friesen, J. Preto, An overview of sub-cellular mechanisms involved in the action of TTFields. International Journal of Environmental Research and Public Health **13**, 1128 (2016).

[6] M. Cifra, J. Pokorny, D. Havelka, and O. Kucera, Electric field generated by axial longitudinal vibration modes of microtubule. Biosystems **100** 2 (2010).

[7] K. A. Thackston, D. D. Deheyn, and D. F. Sievenpiper, Simulation of electric fields generated from microtubule vibrations. Phys. Rev. E **100**, 022410 (2019).

[8] E. Prodan and C. Prodan, Topological phonon modes and their role in dynamic instability of microtubules. Phys. Rev. Lett. **103**, 24 (2009).

[9] Y. M. Sirenko, M. A. Stroscio, and K. W. Kim, Elastic vibration of a microtubule in a fluid. Phys. Rev. **53**, 1 (1996).

[10] S. Portet, J. A. Tuszynski, C. W. V. Hogue, and J. M. Dixon, Elastic vibrations in seamless microtubules. Eur. Biophys. Journal **34**, 912-920 (2005).

[11] S. Li, C. Wang, and P. Nithiarasu, Three-dimensional transverse vibration of microtubules. J. of Appl. Phys. **121**, 234301 (2017).

[12] A. A. Aslam and C. Prodan, Experimentally measured phonon spectrum of microtubules. J. Phys. D: Appl. Phys. **53**, 025401 (2020).

[13] E. Kirson et al. Alternating electric fields arrest cell proliferation in animal tumor models and human brain tumors. PNAS **104** 24 (2007)

[14] M. S. Dresselhaus and P. C. Eklund, Phonons in carbon nanotubes Advances in Physics **49**:6, 705-814 (2010).

[15] D.J. Bergman, The dielectric constant of a simple cubic array of identical spheres. Journal of physics C: Solid state physics **12**, 22 (1979).

[16] D. J. Bergman, Perfect imaging of a point charge in the quasistatic regime. Phys. Rev. A **89**, 015801 (2014).

[17] A. Farhi and D.J. Bergman, Eigenstate expansion of the quasistatic electric field of a point charge in a spherical inclusion structure. Phys. Rev. A **96**, 043806 (2017).

[18] L. Ge, Y. Chong, and A. D. Stone, Steady State ab initio laser theory: Generalizations and analytical results. Phys. Rev. A **82**, 063824 (2010).

[19] Solar, Max and Buehler, Markus J, Comparative analysis of nanomechanics of protein filaments under lateral loading. Nanoscale **4** 4 pp. 1177-1183 2012, Royal Society of Chemistry

[20] L. D. Landau and E. M. Lifshitz, Electrodynamics of Continuous Media, 2nd Edition, Pegamon Press, Chapter XVI.

[21] J. B. Pendry, Nagative refraction makes a perfect lens. Phys. Rev. Lett. **85**, 3966 (2000).

[22] G. Edwards, D Hochberg, and TW Kephart, Structure in the electric potential emanating from DNA. Phys. Rev. E **50**, R698(R) (1994).

[23] D.J. Bergman, Electromagnetic eigenstates of finite cylinders and cylinder-clusters: application to macroscopic response of meta-materials. Proc. SPIE 7032, Plasmonics: Metallic Nanostructures and Their Optical Properties VI, 70321A (2008).

[24] M. S. Dresselhaus, G. Dresselhaus, A. Jorio, A. G. Souza Filho, M. A. Pimenta, and R. Saito, Single Nanotube Raman Spectroscopy. Acc. Chem. Res. **35**, 1070-1078 (2002).

[25] C. P. Kittel and P. McEuen, Introduction to solid state physics. Vol. 8. Wiley New York (1976), Chapters 4 and 10.

[26] V. M. Agranovich, and V. Ginzburg, Crystal optics with spatial Dispersion, Springer Series in Solid-State Sciences, 42 (1979).

[27] A. V. Shchegrov, K. Joulain, R. Carminati, and J. J. Greffet, Near-Field Spectral Effects due to Electromagnetic Surface Excitations. Phys. Rev. Lett. **85**, 7 (2000).

[28] K. L. Kliewer and R. Fuchs, Optical Modes of Vibration in an Ionic Crystal Slab Including Retardation. I. Nonradiative Region. Phys. Rev. **144**, 2 (1965).

[29] R. H. Dicke, Coherence in spontaneous radiation processes. Phys. Rev. **93**, 99 (1954).

[30] W. L. Lama, R. Jodoin, and L. Mandel, Superradiance in radiatively coupled tuning forks. American Journal of Physics **40**, 32 (1972).

[31] J. C. Kimball and C. Y. Fong, Anharmonicity, phonon localization, two-phonon bound states, and vibrational spectra. Phys. Rev. B **23**, 4946 (1981).

[32] C. Hess and M. Wolf, and M. Bonn, Direct observation of vibrational energy delocalization on surfaces: CO on Ru(001). Phys. Rev. Lett. **85**, 4341 (2000).

[33] M. Gonzalez-Jimrenez, et al., Observation of coherent delocalized phonon-like modes in DNA under physiological conditions. Nat. Comm. **7**, 11799 (2016).

[34] S. Sahu, S. Ghosh, B. Ghosh, K. Aswani, K. Hirata, D. Fujita, and A. Bandyopadhyay, Atomic water channel controlling remarkable properties of a single brain microtubule: Correlating single protein to its supramolecular assembly. Biosensors and Bioelectronics. **47**, (2013).

[35] R. Tao, Z. Chen, and P. Sheng, First-principles Fourier approach for the calculation of the effective dielectric constant of periodic composites. Phys. Rev. B **41**, 4 (1990).

[36] D. J. Bergman, K. J. Dunn, Bulk effective dielectric constant of a composite with a periodic microgeometry. Phys. Rev. B **45**, 23 (1992).

[37] G. N. Milton, R. C. McPhedran, and D. R. McKenzie, Transport properties of arrays of intersecting cylinders. Appl. Phys. **25**, 23 (1981).

[38] R. C. McPhendran and D. R. McKenzie, The conductivity of lattices of spheres I. The simple cubic lattice. Proc. R. Soc. London, Ser. A **359**, 45 (1978).

[39] A. Yariv and P. Yeh, Optical Waves in Crystals, John Wiley and Sons (1984).

[40] R Ruppin and R Englman, Optical phonons of small crystals. Rep. Prog. Phys. **33**, 149 (1970).

[41] C. F. Bohren and A. J. Hunt, Scattering of electromagnetic waves by a charged sphere. Canadian Journal of Physics **55**, 21 (1977).

[42] R. L Heinisch, F.X. Bronold, and H. Fehske, Mie scattering by a charged dielectric particle. Phys. Rev. Lett. **109**, 243903 (2012).

[43] J. Preto, Semi-classical statistical description of Frohlich condensation. J. Biol. Phys. **43** 167-184 (2017).

[44] R. Hillenbrand, T. Taubner, and F. Keilmann, Phonon-enhanced light-matter interaction at the nanometre scale. Nature **418**, 159 (2002).

[45] R. H. Ritchie, Plasma Losses by Fast Electrons in Thin Films. Phys. Rev. **106**, 874 (1957).

[46] M. Jablan, H. Buljan, and M. Soljacic, Plasmonics in graphene at infrared frequencies. Phys. Rev. B **80**, 245435 (2009).

[47] N. Rivera, I. Kaminer, B. Zhen, J. D. Joannopoulos, M. Soljacic, Shrinking light to allow forbidden transitions. Science **353**, 29 (2016).

[48] Z. Fu and M. Yamaguchi, Coherent Excitation of Optical Phonons in GaAs by Broadband Terahertz Pulses. Sci. Rep. **6**:38264 (2016).

[49] I. Minoura and E. Muto, Dielectric Measurement of

Individual Microtubules Using the Electroorientation Method. Biophysical Journal **90**, 3739-3748 (2006).

[50] M. D. Anderson, et. al, Two-Color Pump-Probe Measurement of Photonic Quantum Correlations Mediated by a Single Phonon. Phys. Rev. Lett. **120**, 233601 (2018).

[51] G. M. Whitesides and B. Grybowski, Self-Assembly at All Scales. Science **295**, 5564 (2002).; G. M. Whitesides and M. Boncheva, Beyond molecules: Self-assembly of mesoscopic and macroscopic components. PNAS **99**, 8 (2002).